Journal of Catalysis 349 (2017) 208–217

Contents lists available at ScienceDirect

Journal of Catalysis

journal homepage: www.elsevier.com/locate/jcat

Facet effect of Pd cocatalyst on photocatalytic CO_2 reduction over g-C_3N_4

Shaowen Cao [a], Yao Li [a], Bicheng Zhu [a], Mietek Jaroniec [b], Jiaguo Yu [a,c,*]

[a] State Key Laboratory of Advanced Technology for Materials Synthesis and Processing, Wuhan University of Technology, Wuhan 430070, PR China
[b] Department of Chemistry and Biochemistry, Kent State University, Kent, OH 44242, USA
[c] Department of Physics, Faculty of Science, King Abdulaziz University, Jeddah 21589, Saudi Arabia

ARTICLE INFO

Article history:
Received 24 December 2016
Revised 4 February 2017
Accepted 6 February 2017

Keywords:
CO_2 photoreduction
Pd cocatalyst
Surface structure
Charge transfer

ABSTRACT

The separation and transfer of charge carriers, adsorption of CO_2 molecules, and desorption of product molecules are crucial factors that affect the CO_2 photoreduction process. Herein, we demonstrate the significant facet effect of Pd cocatalyst toward CO_2 photoreduction over graphitic carbon nitride (g-C_3N_4). The surface atomic structure of Pd cocatalyst can be precisely controlled by adjusting the amount of {1 1 1} and {1 0 0} facets to modulate the interfacial charge carrier transfer, CO_2 adsorption and CH_3OH desorption. It is shown that the tetrahedral Pd nanocrystals with exposed {1 1 1} facets function as a more efficient cocatalyst as compared to cubic Pd nanocrystals with exposed {1 0 0} facets, which is reflected by enhancing the CO_2 photoreduction over graphitic carbon nitride. The origin of such remarkable shape-induced effect is explained on the basis of experimental studies of charge transfer dynamics and the atomic-scale DFT modeling of CO_2 adsorption and CH_3OH desorption.

1. Introduction

The rapid consumption of fossil fuels has led to a significant increase of emitted carbon dioxide (CO_2) into the atmosphere, consequently causing not only the global energy shortage but also a serious greenhouse effect [1–3]. To balance the global carbon cycle and slow down the energy crisis, the conversion of CO_2 into sustainable hydrocarbon fuels is a potentially promising strategy [4–6]. However, the high thermodynamic stability of the CO_2 molecule requires a high input of energy and efficient catalysts to break the C=O bond during the conversion process [7]. Therefore, the photocatalytic reduction of CO_2 into hydrocarbon fuels with utilization of renewable solar energy has emerged as an effective means of low energy cost [8–10].

Metal nanoparticles are frequently used as efficient catalysts in many important reactions [11–13]. The surface facets of metal nanoparticles strongly affect the catalytic activity due to the diverse arrangement of surface atoms, which usually serve as predominant active sites [14–17]. In photocatalysis, metal nanoparticles act as cocatalysts to enhance the performance of photocatalysts for reactions such as H_2 evolution and CO_2 reduction, by facilitating the charge separation, lowering the activation energy and reducing the overpotential [18–20]. However, these metal nanoparticles are normally deposited on the surface of photocatalysts by in-situ photodeposition or impregnation methods, leading to the formation of an irregularly spherical shape. Hence it is challenging to precisely probe the effects of surface atomic structure of metal cocatalysts on the photocatalytic activity. Importantly, the surface atomic structure of metal cocatalysts is expected to have a significant impact on the molecular absorption and charge separation in photocatalytic reactions [21–23]. Therefore, it is indispensable to investigate the shape effects of metal cocatalysts by rational methods for designing a highly efficient photocatalytic system.

Graphitic carbon nitride (g-C_3N_4) is a promising photocatalyst with high stability, appropriate electronic structure and excellent light absorption ability [24,25]. The conduction band position of g-C_3N_4 is much more negative than the reduction potentials of CO_2 to various hydrocarbon fuels, thus in recent years g-C_3N_4 has attracted a lot of attention in the field of photocatalytic CO_2 reduction [26,27]. Very recently, density functional theory (DFT) calculations have revealed that a strong interaction could occur between Pd atoms and the lone-pair electrons of the neighbouring pyridinic nitrogen atoms of g-C_3N_4 [28]. Hence, in this work, we employ g-C_3N_4 as the model photocatalyst and demonstrate a remarkable shape-induced effect of Pd cocatalyst on g-C_3N_4 photocatalyst towards photocatalytic CO_2 reduction. Cubic and tetrahedral Pd nanoparticles with different exposed facets can be precisely synthesized and ex-situ deposited onto the surface of g-C_3N_4 via elec-

---

* Corresponding author at: State Key Laboratory of Advanced Technology for Materials Synthesis and Processing, Wuhan University of Technology, Wuhan 430070, PR China. Fax: +86 27 87879468.

E-mail address: jiaguoyu@yahoo.com (J. Yu).

http://dx.doi.org/10.1016/j.jcat.2017.02.005
0021-9517/

trostatic assembly. The photocatalytic CO_2 reduction performance is found to be highly sensitive to the surface atomic structure of Pd nanoparticles due to the different charge transfer ability, adsorption energy of CO_2 molecules and desorption energy of CH_3-OH molecules.

2. Experimental and computational methods

2.1. Materials

Urea (98.0%), Na_2PdCl_4 (99.99%), Pd(acac)$_2$ (99.0%), poly vinyl pyrrolidone (PVP, MW ≈ 1,300,000), L-ascorbic acid (AA, 99.0%), KBr (99.0%), diglycol (DEG, 99.0%), tetraethylene glycol (TTEG, 90%) and ethylene glycol (EG, 99.0%) were all purchased from Sigma–Aldrich and used as received without further purification. Deionized (DI) water was used for all experiments.

2.2. Preparation of bulk g-C_3N_4

g-C_3N_4 was prepared by thermal treatment of urea [29]. Typically, 70 g of urea powder was put into an alumina crucible with a cover, and heated in a muffle furnace at 500 °C for 2 h with a heating rate of 5 °C/min. The resultant g-C_3N_4 yellow powder (CN) was collected for use without further treatment.

2.3. Preparation of different shapes of Pd nanoparticles

The Pd nanocubes (NCs) and nanotetrahedrons (NTs) were prepared by using the slightly modified methods reported previously [30,31]. For the synthesis of Pd NCs [30], 105 mg of PVP, 60 mg of AA and 500 mg of KBr were dissolved in 8.0 mL of deionized water at ambient temperature. The mixture was placed in a home-made 50 mL capped glass vial and pretreated in an oil bath at 80 °C for 10 min under vigorous stirring. Then, the reaction was maintained at 80 °C for 3 h after rapid injection of 3.0 mL of Pd-containing aqueous solution (57 mg of Na_2PdCl_4).

Pd NTs were synthesized using a seed-mediated approach [30,31]. For the synthesis of cuboctahedral Pd seeds, 2.0 mL of EG containing 30 mg of PVP was introduced into a 20 mL glass vial and preheated in an oil bath at 160 °C for 10 min under vigorous stirring. Then, the reaction was maintained for 3 h after rapid injection of 1.0 mL of Pd-containing EG solution (15.5 mg of Na_2PdCl_4). The product was quenched by ice-water bath for 15 min after the vial was removed from the oil bath. The seeds were washed three times with acetone, *n*-hexane and ethanol and then re-dispersed in 2.5 mL of EG. Afterward, 3.0 mL of TTEG containing 10 mg of PVP and 0.1 mL of EG containing 0.2 mg of cuboctahedral Pd seeds were placed in a home-made 50 mL glass vial with a reflux condenser. Then, the reaction temperature was maintained at 140 °C for 1 h after rapid injection of 0.5 mL of Pd-containing TTEG solution (2.1 mg of Pd(acac)$_2$).

Both the products were quenched by maintaining in an ice-water bath for 30 min, and washed several times with acetone, *n*-hexane and DI water to remove the solvent, excess of PVP (PVP was employed as a dual-function agent to reduce the Pd precursor with its hydroxyl end groups as well as to stabilize the Pd nanocrystals) [32] and other ions by centrifugation. The products were collected and stored in pure ethanol, keeping the same concentration (2 mg mL^{-1}) for further usage and characterization.

2.4. Preparation of Pd/g-C_3N_4 hybrid photocatalysts

As shown in Fig. 1, the Pd/g-C_3N_4 hybrid photocatalysts were synthesized via electrostatic assembly of Pd nanoparticles onto the surface of g-C_3N_4. Typically, 300 mg of CN powder and 1.5 mL of Pd nanoparticles-containing ethanol solution were dispersed in 200 mL of DI water by ultrasonication for 3 h to obtain a suspension. After that, the pH of the mixed suspension was adjusted to 2.5 (the zeta potentials of CN and Pd nanoparticles suspensions at pH = 2.5 are 30.4 mV and −0.232 mV, respectively) with HCl solution (0.5 M) under vigorous stirring. The suspension was kept under stirring for 1 h and sonicated for 2 h. The obtained precipitates were washed with DI water for 3 times and dried in an oven at 80 °C overnight. The obtained different shapes of palladium (Pd NCs and NTs) coupled with g-C_3N_4 photocatalysts were denoted as C—CN and T—CN, respectively. In order to eliminate the influence of the synthesis process on the photocatalytic performance, the same treatment process was applied to prepare CN without Pd nanoparticles, and the obtained product was denoted as CN1.

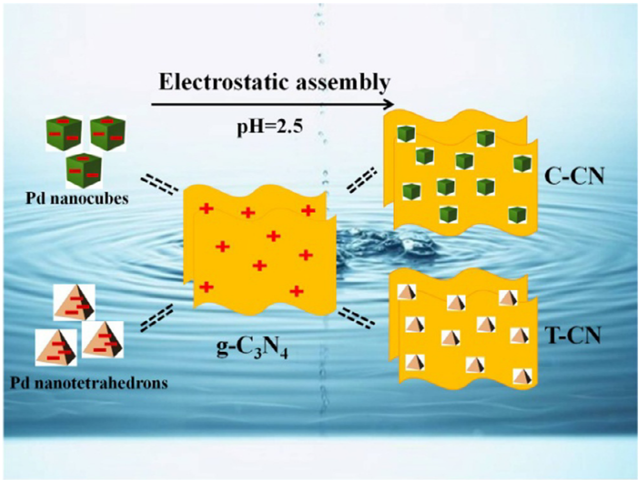

Fig. 1. Schematic illustration of the process used for the synthesis of Pd/g-C_3N_4 hybrids.

2.5. Characterization

The X-ray diffraction (XRD) measurements were carried out on an X-ray diffractometer (Rigaku, Japan) with Cu Kα radiation at a scan rate (2θ) of 0.05° s^{-1}, and the accelerating voltage and applied current were 40 kV and 80 mA, respectively. Transmission electron microscopy (TEM) and high-resolution TEM (HRTEM) images were recorded by using a JEOL JEM-2100F electron microscope, working at an accelerating voltage of 200 kV. X-ray photoelectron spectroscopy (XPS) measurements were performed on an ultra-high-vacuum VG ESCALAB 210 electron spectrometer with an Al Kα source. All the binding energies were referenced to the C1s peaks at 284.8 eV of the surface adventitious carbon. UV–visible diffuse reflectance spectra (DRS) were obtained by using a UV–visible spectrometer (UV-2600, SHIMADZU, Japan) in the wavelength range of 200–800 nm, with $BaSO_4$ as the reference standard. The concentrations of Pd in the prepared Pd/g-C_3N_4 structures were determined by the inductively coupled plasma atomic emission spectrometry (ICP-AES) (PerkinElmer, Optima 4300DV, American) after dissolving the particles with aqua regia. The Fourier transform infrared spectra (FTIR) of the samples were recorded on an IRAffinity-1 FTIR spectrometer in a KBr pellet, scanning from 400 to 4000 cm^{-1} at room temperature. The Brunauer–Emmett–Teller (BET) specific surface areas (S_{BET}) were measured by a multipoint BET method using adsorption data obtained on a Micromeritics ASAP 3020 nitrogen adsorption apparatus (USA). Pore size distributions were obtained by the Barrett–Joyner–Halenda (BJH) method using nitrogen desorption data. The pore volume was calculated